JOINT EUROPEAN TORUS JET

JET–P(93)107

K. Barrass, G. Janeschitz

Estimation of the Maximum Divertor Radiative Fraction in the Presence of a Neutral Cushion

Estimation of the Maximum Divertor Radiative Fraction in the Presence of a Neutral Cushion

K. Barrass, G. Janeschitz[1]

JET-Joint Undertaking, Culham Science Centre, OX14 3DB, Abingdon, UK

[1]Present affiliation: ITER-EDA, ITER Joint Working Site,
Max-Planck-Institut fiir Plasmaphysik, Garching, Munich, Germany

Preprint of a paper to be submitted for publication in Nuclear Fusion
January 1994

ESTIMATION OF THE MAXIMUM DIVERTOR RADIATIVE FRACTION IN THE PRESENCE OF A NEUTRAL CUSHION

K. BORRASS, G. JANESCHITZ*
JET Joint Undertaking,
Abingdon, Oxfordshire,
United Kingdom

ABSTRACT. Divertor impurity radiation is considered as one possibility to reduce the target heat load in ITER-grade devices to acceptable values. The radiative power fraction in the divertor is, however, in principle limited and under standard high recycling conditions too small to achieve this goal. In this paper we discuss the possible increase of the maximum radiative fraction by a "neutral cushion" that provides a pressure drop in the divertor by ion-neutral interaction. A pressure drop by about a factor of ten would allow the radiative fraction to increase sufficiently to satisfy constraints on ITER target loads. Experimental and theoretical evidence has been given in the literature for gas targets with the required properties. Supersonic flow conditions at the target are also included in the discussion, but are found to be insufficient, by themselves, to provide the required effect.

1. INTRODUCTION

Previous divertor concepts for next-generation devices mainly relied on the so called high recycling regime, originally developed for INTOR [1]. In this regime the energy balance in the divertor is dominated by hydrogen recycling which occurs in a thin layer in front of the plate. While a sizable fraction of the incoming power is consumed by the recycling process, much of it is redeposited onto the plate by recombination or radiated onto the plate because of the close proximity of the recycling region to the plate. While the high recycling solution was marginally acceptable for relatively small, low powered devices like INTOR or ITER CDA [1, 2], it fails in the size and power regime ($2 - 4$ MW) envisaged for ITER EDA.

Novel concepts have been proposed, which crudely can be divided into cases where (i) the plasma extinguishes before reaching a target due to volume recombination [3] and cases where (ii) the plasma stays in contact with a plate, but a low electron temperature "neutral cushion" region develops in front of the target which is dominated by cx and $i - n$ collisions. In this case ionization occurs in a separate ionization front outside the cushion.

A cushion may have a variety of effects among which momentum and energy losses of the divertor plasma (direct or by neutral induced transport) are of particular interest. While the potential of cx and $i - n$ induced processes for sufficient energy removal [4] still has to be demonstrated, there is convincing experimental and theoretical evidence for momentum losses (pressure drop along field lines) induced by a neutral cushion [5, 6, 7].

For all concepts enhanced impurity radiation from the divertor by seeding of recycling impurities with favourable radiation characteristics, is considered as a supporting possibility. In this context it is a widespread belief that a sufficiently high impurity radiative fraction would solve the power exhaust problem even in a high recycling divertor. In this paper we emphasize that, apart from the question whether the required impurity concentrations can be maintained without spoiling the performance of the machine (ignition, burn length), the SOL impurity radiative fraction cannot be chosen freely. In particular, the maximum

**Present affiliation:* *ITER EDA, ITER Joint Working Site, Max-Planck-Institut für Plasmaphysik, Garching/Munich, Germany*

allowable radiative fraction is much too low under ITER EDA conditions to reduce the target load to acceptable levels in the normal high recycling regime. However, the radiative fraction can be enhanced, if a cushion provides an extra pressure drop along field lines. Therefore, the cushion solutions, even if they do not provide a direct means for energy removal from the divertor plasma, are essential for efficient power removal by enhanced impurity radiation.

The mechanism leading to the limitation is related to the boundary conditions at the plate. For high radiative fractions the plasma flow at the target may become supersonic and the traditional boundary condition, which assumes $M = 1$ at the sheath entrance, is then inappropriate. In this paper we therefore allow for arbitrary Mach numbers.

The limit for impurity divertor radiation has been first described in Ref. [8] for the standard high recycling regime and the standard boundary condition. This paper follows similar lines, but includes the effect of a cushion induced pressure drop, of supersonic flow at the sheath, and the impact of different scalings of perpendicular transport in the SOL. Also, scalings are derived which relate the machine and discharge parameters with the maximum radiative fraction and the achievable pressure drop. Numerical results are given for ITER EDA parameters.

2. BASIC 2-POINT MODEL EQUATIONS

The discussion is performed within the framework of a two-point SOL model. A version of the basic equations of a two point model are given in Refs [9, 10] for the case of Bohm-like perpendicular heat transport, which is used in slightly modified form to allow for supersonic flow at the sheath entrance and generalized perpendicular heat transport ($_S$, $_D$ denote stagnation point and divertor quantities, respectively) [1]

$$n_D = \frac{f_P}{1+M_D^2}\frac{n_S T_S}{T_D} \qquad (1)$$

$$\Delta = \frac{5}{32}\frac{c}{e}\frac{n_S T_S^2 F}{q_\perp B_t} \qquad (2)$$

$$T_S = \left(\frac{49}{4\kappa}\frac{q_\perp L^2}{\Delta}\right)^{2/7} \qquad (3)$$

[1]The units are cgs units except where otherwise stated.

$$\frac{7}{2}\frac{L(1-f_{imp})q_\perp}{\Delta} = c_s n_D M_D(\xi + (\gamma' + M_D^2)T_D) \qquad (4)$$

Here Δ is the temperature SOL thickness, L the connection length and $q_\perp$ the mean power flux across the separatrix. M_D is the Mach number at the target. f_{imp} is the SOL impurity radiative fraction, while f_P reflects a possible pressure drop along the field lines due to ion-neutral interaction or other momentum loss mechanisms. $f_P = 1$ in the absence of momentum losses. Otherwise the notation is conventional. Equation (1) is derived from the momentum balance equation. Equations (2) and (3) follow from local analysis of the SOL power balance, while Eq. (4) is essentially the global power balance equation at the target.

To generalize the transport model used in Ref. [9], we adopt the general format for the heat diffusivity $\chi_\perp$ that has evolved in the scale invariant approach to confinement scaling [11]

$$\chi = D_B F(\rho^*, ...) \qquad (5)$$

Here D_B is the Bohm diffusivity and ρ^* the normalized Larmor radius. F is a function which depends, apart from ρ^*, on other dimensionless quantities which describe the effects that determine the transport. The generalized transport according to Eq. (5) is easily implemented into the basic equations given in Ref. [9] for Bohm-like perpendicular transport by making the substitution $B_t \longrightarrow B_t F^{-1}$.

The Bohm criterion requires $M_D \geq 1$ at the sheath entrance. Traditionally the condition $M_D = 1$ has been adopted as boundary condition for SOL fluid models. However, it has become evident that this restriction may be inappropriate, particular in cases where $M > 1$ in upstream regions. We therefore allow for arbitrary values of M_D. In this case the energy flux onto the target is given by $q_{\|,D} \simeq c_s n_D M_D(\gamma' + M_D^2)T_D$, where $\gamma' = \gamma - 1$ and γ is the usual sheath transmission factor [12, 13].

In Eqs (1) to (4) it is implicitly assumed that the presence of the cushion does not lead to additional terms in the energy balance Eq. (4). Also, as in 2-P models in general, the temperature T_0 at the entrance of the ionization region has to be sufficiently small so that $(1-(T_0/T_S)^{7/2})^{2/7} \simeq 1$ [9].

f_P and f_{imp} are considered as externally controllable parameters. Control of f_{imp} has to be achieved by properly adjusting the injection rate of the seed impurity. The formation of the cushion

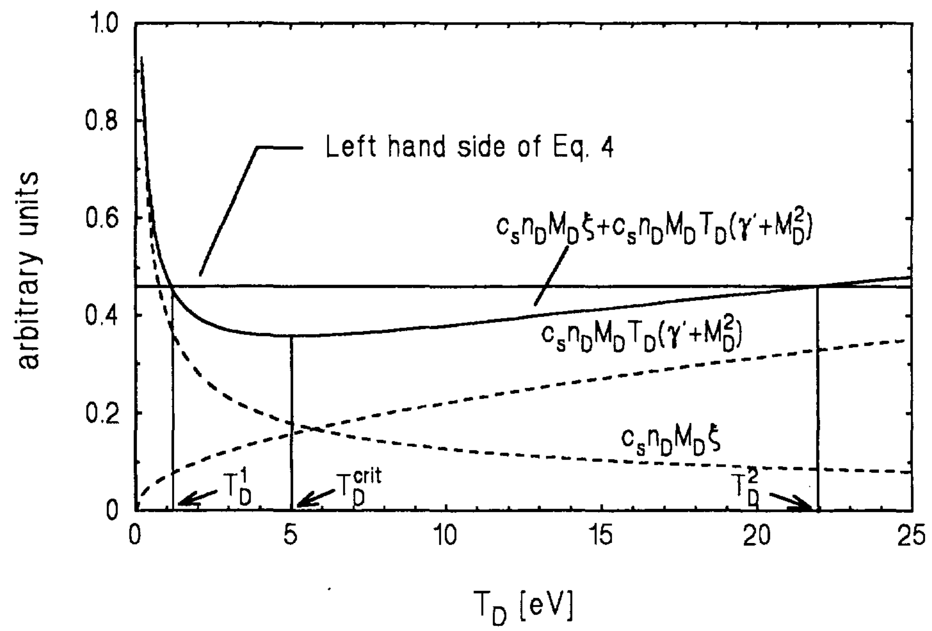

FIG. 1. *Terms of the energy balance Eq. (4) versus T_D at fixed $q_\perp$, n_S and for $f_P = 1$ and $M_D = 1$.*

and hence f_P have to be adjusted by tailoring the discharge. The question, whether this is possible and how it has to be done, has to be answered within the framework of the cushion theory. M_D is also treated as a parameter the impact of which will be shown to be negligible in the present context. Therefore, M_D can be left undetermined.

For a detailed discussion of Eqs (1) to (4) see Refs [9, 10]. While these equations have to be solved numerically in general, some essential conclusions can be inferred analytically.

3. ANALYTICAL CONSIDERATIONS

3.1 Heuristic Discussion

We start with a heuristic derivation of the condition that leads to a limitation of f_{imp}. In this discussion, in order to make the underlying physics transparent, we assume the upstream conditions (i.e. n_S and $q_\perp$) to be fixed. Under these conditions also the upstream pressure is determined. In fact, combining Eqs (2) and (3), one gets

$$T_S \propto \frac{q_\perp^{4/11} B_t^{2/11} L^{4/11}}{n_S^{2/11} F^{2/11}} \tag{6}$$

Hence, for given $q_\perp$ and n_S, also T_S (and consequently $n_S T_S$) are determined, independently of f_{imp}, f_P, M_D and T_D. Thus, the upstream pressure is not affected by the radiative fraction, the presence of a cushion or the downstream boundary condition. This implies, in particular, that, for given $q_\perp$ and n_S, the scaling

$$n_D = \frac{f_P}{1+M_D^2}\frac{n_S T_S}{T_D} \propto \frac{f_P}{1+M_D^2}\frac{1}{T_D} \tag{7}$$

holds. Hence, the right-hand side terms of the energy balance Eq. (4) scale as (In the analytical discussion we ignore the weak temperature and density dependence of ξ [14] and assume $\xi \simeq const$)

$$c_s n_D M_D \xi \propto \frac{M_D f_P}{1+M_D^2} T_D^{-1/2} \propto T_D^{-1/2} \tag{8}$$

and

$$(\gamma' + M_D^2) T_D c_S n_D M_D \propto \frac{M_D f_P (\gamma' + M_D^2)}{1+M_D^2} T_D^{1/2}$$

$$\propto T_D^{1/2} \tag{9}$$

Figure 1 shows the various terms of Eq. (4) versus T_D (at constant $q_\perp$ and n_S and fixed f_P and M_D). The behaviour is obvious from Eqs (8) and (9). Obviously the right-hand side has a minimum and a solution can only exist if (T_D^{crit} is the temperature at the minimum)

$$\frac{7}{2}\frac{L q_\perp}{\Delta}(1 - f_{imp}) \geq c_s(T_D^{crit}) n_D(T_D^{crit}) M_D \xi +$$

$$+c_s(T_D^{crit})n_D(T_D^{crit})T_D^{crit}M_D(\gamma' + M_D^2)) \qquad (10)$$

holds, i. e., if the power into the divertor exceeds the minimum losses. T_D^{crit} is determined by the condition

$$\frac{\partial G}{\partial T_D} = 0$$

where

$$G(T_D, M_D, \xi, \gamma') = \frac{M_D}{1 + M_D^2} \frac{\xi + T_D(\gamma' + M_D^2)}{T_D^{1/2}}$$

One gets

$$T_D^{crit} = \xi/(\gamma' + M_D^2) \qquad (11)$$

resulting in

$$G(T_D^{crit}, M_D, \xi, \gamma') = 2\sqrt{\xi\gamma'} \frac{M_D\sqrt{1 + M_D^2/\gamma'}}{1 + M_D^2} \qquad (12)$$

Obviously

$$\lim_{M_D \to \infty} G(T_D^{crit}, M_D, \xi, \gamma') = 2\sqrt{\xi} \qquad (13)$$

and

$$\frac{G(T_D^{crit}, M_D = 1, \xi, \gamma')}{G(T_D^{crit}, M_D = \infty, \xi, \gamma')} = \frac{\sqrt{\gamma}}{2} = \sqrt{2} \qquad (14)$$

if $\gamma = 8$ is adopted [14], i.e., the dependence on M_D is weak.

Some additional remarks may help to interpret this result:

- The limit basically arises through the fact that, for given upstream conditions, the sum of the losses provided by recycling and the power flux into the sheath cannot drop below a minimum.
- A cushion reduces, at given upstream conditions, the divertor loss terms by decreasing the target plate density n_D (see Eq. (7)), thus allowing higher radiative fractions in the SOL (reduction of the left-hand side of Eq. (10)).
- Supersonic flow at the sheath entrance ($M_D > 1$) has, in principle, the same effect (see Eq. (1)), but the decrease of n_D is counteracted by the increase of kinetic energy transported into the sheath (see Eq. (9)).
- In general, and if inequality holds in Eq. (10), there are two solutions at temperatures T_D^1 and T_D^2. Only the upper one (at T_D^2) is thermally stable, while the lower one (at T_D^1) is unstable. These aspects have been discussed in detail in Ref. [9].
- In reality only the range $T_D \geq T_D^{crit}$ is accessible. Once the critical point is reached by approaching it through a sequence of stable solutions, the temperature would collapse, until eventually a temperature regime is reached where the basic equations are no longer valid. We come back to this point in the discussion.

3.2 General Form of the Limit

The assumption of fixed upstream parameters, made for illustrative purposes, can be abandoned. Eliminating Δ, T_S and n_D from Eqs (1) to (4), one gets

$$\frac{1 - f_{imp}}{f_P} \frac{q_\perp^{10/11}}{n_S^{16/11}} = c\frac{L^{1/11}F^{5/11}}{B_t^{5/11}} G(T_D, M_D, \xi, \gamma')$$

$$\geq c\frac{L^{1/11}F^{5/11}}{B_t^{5/11}} G(T_D^{crit}, M_D, \xi, \gamma') \qquad (15)$$

where c is a constant. Equation (15) generalizes Eq. (10) and casts it into a more convenient form. It is a constraint on the seven quantities f_P, f_{imp}, M_D, n_S, $q_\perp$, B_t and L. Taking six of them as given, it establishes an upper (or lower) limit on the seventh one.

If, for instance, f_P, f_{imp}, M_D, B_t, L and $q_\perp$ are given, it provides an upper limit for the upstream density (density limit). This aspect has been previoulsly discussed in Refs [15, 9]. The limit is decreased by increasing f_{imp}, while it is increased by reducing f_P.

Taking Eq. (15) with the equality sign, prescription of six variables gives the critical (maximum or minimum) value for the seventh one and the corresponding solution of Eqs (1) to (4) is the marginal case where $T_D = T_D^{crit}$.

A general consequence of Eq. (15) is that, although the impurity radiative fraction can never reach 100%, f_{imp} can be arbitrarily close to unity if f_P is sufficiently low. In order to make more specific statements, one has to reduce the parameter space by confining to special cases (see Sec. 4)

3.3 Target Loads

Our main interest is the potential of divertor impurity radiation to reduce the target heat load q_t, which has the following general form

$$q_t = M_D n_D c_s \times$$
$$\times\left[(\gamma' + M_D^2)T_D + \xi_{ion} + \frac{\xi - \xi_{ion}}{2}\right]sin\psi \qquad (16)$$

where ψ is the B-field pitch. The first term in Eq. (16) describes the power flux into the sheath region. The second term gives the power load onto the plate which is associated with the release of the ionization energy at recombination. $\xi - \xi_{ion}$ is the power radiated per ionization event. Assuming a thin recycling layer in front of the plate, half of this power is absorbed within the plate (third term).

The previous considerations provide a scaling relation for the minimum target load q_t^{min}. From Eq. (6) one gets

$$n_s T_S \propto q_\perp^{4/11} B_t^{2/11} L^{4/11} n_S^{9/11} F^{-2/11} \qquad (17)$$

Combining Eqs (1) and (17), one can eliminate n_D from Eq. (16) to get

$$q_t \propto f_P q_\perp^{4/11} n_S^{9/11} B_t^{2/11} L^{4/11} F^{-2/11}$$
$$\times\, G\left(T_D, M_D, \xi_{ion} + \frac{\xi - \xi_{ion}}{2}, \gamma'\right) \qquad (18)$$

It is easy to see that $q_t(T_D) \geq q_t(T_D^{crit})$ for typical values of ξ. Hence, the minimum possible target load dependes weakly on $q_\perp$ and is independent of f_{imp}. Note, however, that in order to reach the minimum, f_{imp} has to adopt its maximum value corresponding to a given f_P. Most important is the strong impact of f_P, which directly illustrates the beneficial effect of a pressure drop induced by a cushion. As with the case of f_{imp} the impact of M_D can be compensated by an f_P variation of not more than 40%.

3.4 Impact of Perpendicular Transport

In order to get an estimation of the impact of different transport models in the parameter regimes of interest, we consider a set of representative scalings and device parameters. We adopt the three generic plasma models given by [11]

$$F = F_0 \rho*^\mu, \ \mu = 1, 0, -1 \qquad (19)$$

where the different values of μ indicate different characteristic length scales λ of the underlying turbulent transport. In particular, $\mu = 1, 0, -1$ correspond to gyro Bohm scaling ($\lambda \approx \rho$), Bohm scaling ($\lambda \approx a$) and stochastic diffusion ($\lambda >> a$), respectively. $F_0 = const$ is assumed (but of course F_0 may depend on μ), thus ignoring possible residual dependencies on other parameters. ASDEX-U, JET and ITER-EDA (see Table I) are chosen as representative small, medium-size and next-generation devices.

TABLE I. REPRESENTATIVE MACHINE PARAMETERS[a]

	R	a	κ	B_t	P_{SOL}
	$[m]$	$[m]$		$[T]$	$[MW]$
ASDEX-U	1.6	0.5	1.6	2.0	6
JET	2.96	1.1	1.68	3.4	25
ITER-EDA	7.75	2.8	1.6	6.0	200

[a] Values are 1994 values and P_{SOL} is estimated on basis of the available heating power and typical bulk radiative fractions.

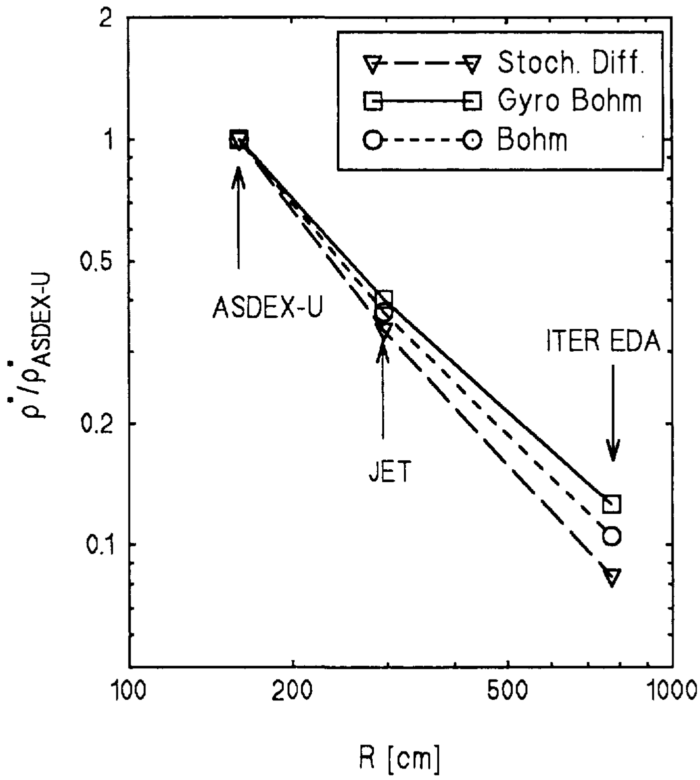

FIG. 2. *Scaling of the normalized gyroradius ρ^* with machine size for different perpendicular transport models and at constant n_S.*

We first derive the scaling of ρ^*. Replacing T_S in

$$\rho^* \propto \frac{T_S^{1/2}}{RB_t} \qquad (20)$$

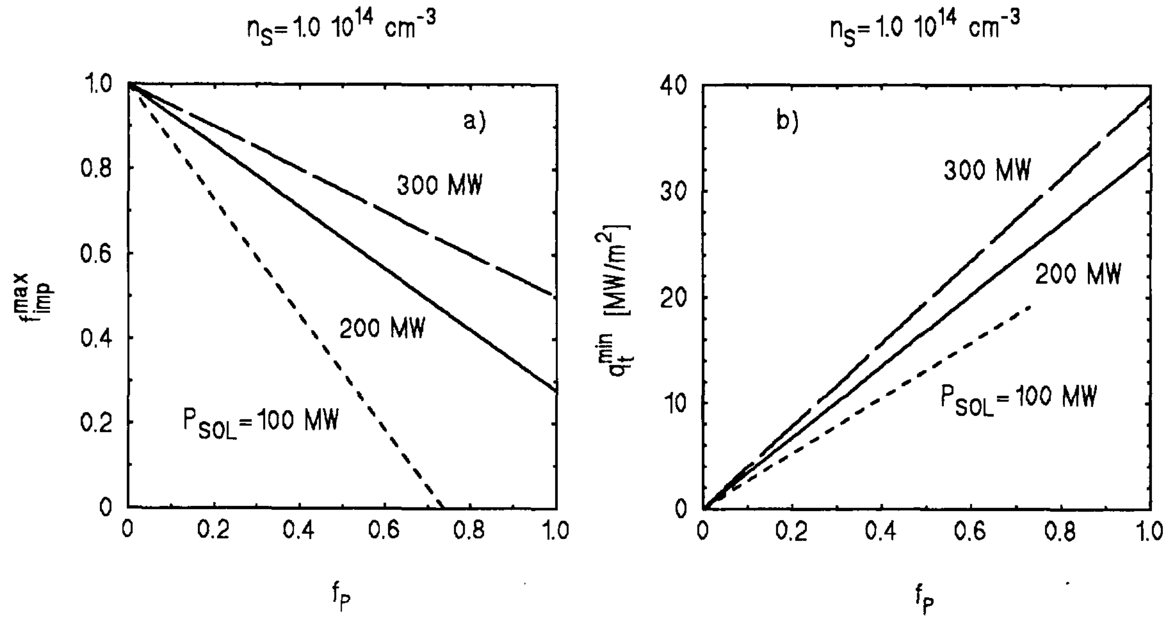

FIG. 3. *Maximum SOL impurity radiative fraction (a) and minimum target load (b) versus pressure reduction factor f_P for ITER-EDA parameters, $n_S = 10^{14}\ cm^{-3}$ and different SOL powers. Bohm-like perpendicular transport ($F \equiv 1$) and $M_D = 1$ have been adopted in both cases. The f_P values required to achieve a certain f_{imp} or q_t value could increase by up to 40% for higher Mach numbers at the target.*

with Eq. (6) and using (19), one gets

$$\rho^* \propto \left(q_\perp^2 n_S R^{-9} B_t^{-10}\right)^{\frac{1}{11+\mu}} \qquad (21)$$

For a specific transport model, even if M_D and f_P are assumed to be given, the parameters of Table 1 do not uniquely determine a set of SOL parameters, but are compatible with different combinations of f_{imp} and n_S. However, the n_S dependence in Eq. (21) is very weak and negligible in the present context. Figure 2 illustrates the range of variation of $\rho^*/\rho^*_{ASDEX-U}$ as following from Eq. (21) for the devices and scalings under consideration. Normalization to ASDEX-U values is justified by the observation that ρ^* values are very similar in present day machines. Together with the scalings it provides information about the changes of ρ^* in ITER.

In order to quantify the impact of transport on q_t^{min}, we also have to know how n_S varies (see Eq. (18)). Since in ITER n_S will be largely determined by bulk plasma related constraints, independently of perpendicular transport, we make the comparison at constant n_S.

Equation (18), (20) and Fig. 2 now provide all information: While in the case of Gyro Bohm scaling ($\mu = 1$) q_t^{min} increases (compared with Bohm scaling), the opposite holds for stochastic diffusion. However, in view of the weak dependence of q_t^{min} on F, the increase/decrease of q_t^{min} does not exceed 50% in either direction.

4. NUMERICAL RESULTS

We now present some results of the numerical treatment of Eqs (1) to (4). As study point we adopt the ITER EDA case of Table 1 with the additional specifications $q_{95\%} = 3$, where $q_{95\%}$ is the safety factor at the 95% flux surface, $n_S = 10^{14}\ cm^{-3}$ and $\sin\psi = 0.07$ (corresponding to an field line-plate angle of 4°, representative of ITER equilibria and non-inclined target plates).

For this particular case Eq. (8) adopts the form

$$\frac{1-f_{imp}}{f_P}\frac{P_{SOL}^{10/11}}{n_S^{16/11}} \geq 17.9 \qquad (22)$$

(n_S in $10^{14}cm^{-3}$, P_{SOL} in MW).

By analogy one obtains for the minimum target heat load

$$q_t^{min} \geq 9.81 f_P P_{SOL}^{4/11} n_S^{9/11} \qquad (23)$$

(q_t in MW/m^2, P_{SOL} in MW, n_S in $10^{14}cm^{-3}$).

From now on we consider Eqs (22) and (23) with the equal sign thus evaluating limiting values. We

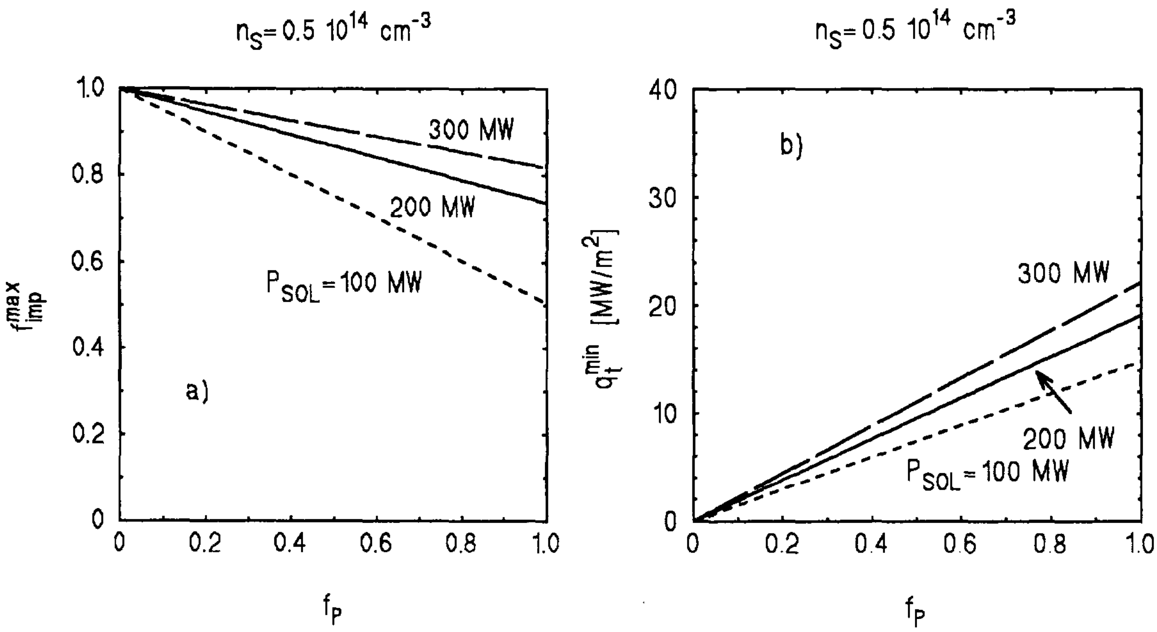

FIG. 4. *Maximum SOL impurity radiative fraction (a) and minimum target load (b) versus pressure reduction factor f_P for ITER-EDA parameters, $n_S = 0.5 \times 10^{14}$ cm^{-3} and different SOL powers. Bohm-like perpendicular transport ($F \equiv 1$) and $M_D = 1$ have been adopted in both cases. The f_P values required to achieve a certain f_{imp} or q_t value could increase by up to 40% for higher Mach numbers at the target.*

also confine to $M_D = 1$ and Bohm-type perpendicular transport.

In Figs 3 and 4, f_{imp}^{max} and q_t^{min} are plotted versus f_P for various values of P_{SOL} and n_S. For the ITER study point of Table 1, assuming the standard high recycling situation ($f_P = 1$), one would have a maximum impurity radiative fraction of less than 30% and a minimum target load of about 30 MW/m^2. A pressure drop of more than an order of magnitude is required to permit radiative fractions (about 90%) that would reduce the target load to values below 5 MW/m^2. Obviously the impact of high Mach numbers or different perpendicular transport is by far too low to have a comparable effect.

It might be surprising that the minimum heat load decreases with decreasing n_S (Figs 3 b) and 4 b)). However, one has to note that q_t^{min} is the target load achieved for the highest possible value of f_{imp}, and that f_{imp} can be higher for lower values of n_S (Figs 3 a) and 4 a)).

5. SUMMARY AND DISCUSSION

The maximum impurity radiative fraction has been evaluated in the presence of a neutral cushion that provides an additional pressure drop $f_P < 1$, but does not affect the energy balance. Basically a limit on f_{imp} arises from the fact that, for given upstream conditions and f_P, the "natural" divertor losses (hydrogen ionization and radiation, power flow into the sheath) cannot drop below a minimum. This limit decreases and correspondingly f_{imp} increases if f_P decreases or the Mach number M_D at the target increases. While the impact of M_D saturates with increasing M_D, f_{imp} can be arbitrarily close to unity if f_P is sufficiently small. The maximum radiative fraction is associated with a minimum of the target load. For ITER-EDA conditions a pressure drop by about a factor of ten is required to reduce the target heat load to acceptable values for $M_D = 1$ and Bohm-like perpendicular transport. Other effects discussed in this paper (supersonic flow conditions, perpendicular transport) have a too weak impact to provide a comparable effect.

Our estimation of the achievable target loads is pessimistic in that it ignores the beneficial effect of a possible poloidal inclination of the plate. On the other hand it is optimistic in that the effect of the unavoidable misalignment of the divertor components, which leads to an increase of the effective target load, is not taken into account. Therefore, our estimation of q_t, based on a perpendicular target, is probably not too far from reality.

The present analysis is limited to cases where T_D^{crit} is sufficiently high ($T_D^{crit} \geq 1.5\ eV$), so that volume recombination is negligible. Because of the flat minimum of G with respect to T_D, even the weak dependence of ξ on n and T may shift T_D^{crit}. For the widely used fit of $\xi(T,n)$ given in Ref. [14], one obtains, for instance, $T_D^{crit} \approx 2 - 3\ eV$ under ITER conditions. Also $M_D > 1$ would shift T_D^{crit} to lower values. However, this does not create a problem. In the presence of a cushion M_D is typically not much above unity (since friction tends to drive the Mach number towars unity,) and in these cases of interest T_D^{crit} should stay in the few eV range. Furthermore, taking the weak dependence of G on T_D, basically all conclusions remain valid if T_D^{crit} is replaced by any $T_D^0 \geq T_D^{crit}$, as long as T_D^0 is "reasonably" close to T_D^{crit}. Here T_D^0 can be, for instance, a temperature set by the requirement of optimum cushion performance.

In a cushion, as it is understood here, ionization is small or negligible. This requires temperatures $T_e < 5\ eV$ consistently with the temperature domain where maximum or near maximum radiative fractions are achieved.

The cushion observed in JET [5] and analyzed in Refs [6, 7] (low density cushion) seems to be one solution with the required properties in that it provides pressure drops of the required size, while its impact on the energy balance is negligible. Also, in order to exist, it requires low power into the cushion, corresponding to radiative fractions in the range of 80-90%.

While in the low density cushion ions are collisional with respect to cx and elastic $i - n$ collisions, neutrals are collisionless. Cushion like solutions are conceivable where also the neutrals are collisional (high density cushion), which are presently under investigation.

In this paper f_{imp} has been always conceived as the impurity radiative fraction, reflecting prime interest in this loss channel. However, f_{imp} may comprise any loss mechanism other than recycling and power flux into the sheath (e.g., heat transport to the walls, cx-losses, etc.) without affecting the basic conclusion of a correlation between the additional losses and a pressure drop. Thus, in particular, gas target solutions where not only momentum but also a major fraction of the incoming energy is removed [4], were also covered by the present analysis.

ACKNOWLEDGEMENTS

The authors gratefully acknowledge stimulating discussions within the JET Divertor Physics Topic Group. Particularly valuable comments on the impact of supersonic flow conditions were made by P. C. Stangeby and J. Wesson.

REFERENCES

[1] International Tokamak Reactor, Phase Two A, Part III, Volume 1, IAEA, Vienna (1991).

[2] ITER Conceptual Design Report, ITER Documentation Series No. **18**, IAEA, Vienna (1991).

[3] PETRAVIC, M., Report PPPL-2912, Princeton Plasma Physics Laboratory, Princeton, N.Y. (1993).

[4] WATKINS, M., L., REBUT, P-H., in Controlled Fusion and Plasma Heating (Proc. 19th Eur. Conf. Innsbruck, 1992), Vol. 16C, Part II, European Physical Society (1992) 731.

[5] JANESCHITZ, G., CLEMENT, S., GOTTARDI, N., et al., in Controlled Fusion and Plasma Heating (Proc. 19th Eur. Conf. Innsbruck, 1992), Vol. 16C, Part II, European Physical Society (1992) 727.

[6] STANGEBY, P. C., Report JET-P(93)13, JET Joint Undertaking, Abingdon, Oxfordshire (1993), accepted for publication in Nuclear Fusion.

[7] BORRASS, K., STANGEBY, P. C., in Controlled Fusion and Plasma Heating (Proc. 20th Eur. Conf. Lisboa, 1993), Vol. 17C, Part II, European Physical Society (1993) 763.

[8] McCRACKEN, G. M., PEDGLEY, J. M., Plasma Phys. Controll. Fusion **35** (1993) 253.

[9] BORRASS, K., Nucl. Fusion **31** (1991) 1035.

[10] BORRASS, K., CAMPBELL, D. J., CLEMENT, S., VLASES, G. C., Nucl. Fusion **33** (1993) 63.

[11] CHRISTIANSEN, J.P., CORDEY J. G., KARDAUN O. J. W. F., THOMSEN K., Nucl. Fusion **31** (1991) 2117.

[12] STANGEBY, P. C., in Physics of Plasma-Wall Interactions in Controlled Fusion (Post, D. E., Behrisch, R., Eds), Plenum Press, New York and London (1986).

[13] CHODURA, R., in Physics of Plasma-Wall Interactions in Controlled Fusion (Post, D. E., Behrisch, R., Eds), Plenum Press, New York and London (1986).

[14] HARRISON, M. F. A., HARBOUR, P. J., HOTSTON, E. S., Nucl. Technol./Fusion **3** (1983) 432.

[15] LACKNER, K., CHODURA, R., KAUFMANN, M., NEUHAUSER, J., RAUH, K. G., SCHNEIDER, W., Plasma Phys. Controll. Fusion **26** (1984) 105.